Environ Fluid Mech (2010) 10:345–368
DOI 10.1007/s10652-009-9134-7

ORIGINAL ARTICLE

Turbulence and turbulent flux events in a small estuary

Mark Trevethan · Hubert Chanson

Received: 17 February 2009 / Accepted: 4 May 2009 / Published online: 21 May 2009

Abstract Relatively little systematic research has been conducted on the turbulence characteristics of small estuaries. In the present study, detailed measurements were conducted in a small subtropical estuary with a focus on turbulent flux events. Acoustic Doppler velocimeters were installed in the mid-estuary at fixed locations and sampled simultaneously and continuously for 50 h. A turbulent flux event analysis was performed for the entire data sets extending the technique of Narasimha et al. (Phil Trans R Soc Ser A 365:841–858, 2007) to the unsteady open channel flow motion and to turbulent sub-events. Turbulent bursting events were defined in terms of the instantaneous turbulent flux. The data showed close results for all ADV units. The very-large majority of turbulent events lasted between 0.04 and 0.3 s with an average of 1 to 4 turbulent events observed per second. A number of turbulent bursting events consisted of consecutive turbulent sub-events, with between 1 and 3 sub-events per main event on average. For all ADV systems, the number of events, event duration and event amplitude showed some tidal trends, with basic differences between high- and low-water periods. A comparison between the present estuary data and the atmospheric boundary layer results of Narasimha et al. (Phil Trans R Soc Ser A 365:841–858, 2007) showed a number of similarities and demonstrated the significance of turbulent events in environmental flows. A burstiness index of 0.85 was found for the present data.

Keywords Turbulence · Turbulent bursting events · Small subtropical estuary · Field measurements · Acoustic Doppler velocimetry · Turbulent sub-events · Turbulent fluxes · Burstiness index · Geophysical flows

M. Trevethan · H. Chanson (✉)
School of Civil Engineering, The University of Queensland, Brisbane , QLD 4072, Australia
e-mail: h.chanson@uq.edu.au

Present Address:
M. Trevethan
MARUM, Centre for Marine Environmental Sciences, The University of Bremen, Bremen 28359, Germany

1 Introduction

While fluctuating turbulence is often represented by its statistical moments, turbulence is not a Gaussian process, in particular in Nature. Many conceptual frameworks and theories are based upon assumptions of quasi-steady state equilibrium, but any turbulent flow is often dominated by coherent structure activities and turbulent events. A turbulent event may be defined as a series of turbulent fluctuations that contain more energy than the average turbulent fluctuations within a studied data section. These turbulent events, often associated with coherent flow structures such as eddies and bursting [15,25], play a major role in terms of sediment scour, transport and accretion as well as contaminant mixing and dispersion ([5,19,20]). Bursting is the quasi-cyclic turbulent energy production in turbulent boundary layers first identified by [15]. There have been many progresses in their physical description in laboratory and in the field. Turbulent event analyses were successfully applied to laboratory open channel flows [17,19], wind tunnel studies [21] and atmospheric boundary layer flows [10,18]. They were however rarely applied to unsteady open channel flows and estuaries.

To date, turbulence studies in natural estuaries have been hampered by a lack of fundamental understanding of the turbulence structure. Past measurements were conducted typically for short-periods, or in bursts, sometimes at low-frequency: e.g. [12,14,28,35]. While a few recent studies attempted to gain some information on the characteristics of fine-scale turbulence (e.g. [24,32,34]), the predictions of turbulent mixing and sediment transport in estuaries can rarely be estimated without exhaustive field data for calibration and validation.

In the present study, it is shown that a turbulent flux event analysis may be successfully applied to a natural estuarine system. A field investigation was conducted in a small estuary in Eastern Australia and the turbulent velocities were recorded continuously and simultaneously at high frequency for 50 h at three sampling locations. The data analysis results, and the variations with time of the turbulent event characteristics, are discussed and compared with atmospheric boundary layer data.

2 Field investigation and instrumentation

A series of detailed turbulence field measurements were conducted in an estuary of Eastern Australia with a semi-diurnal tidal regime (Table 1). The estuarine zone was 3.8 km long, about 1 to 2 m deep mid-stream (Fig. 1a). The estuary was a narrow, elongated and meandering channel, with a cross-section which deepens and widens towards the mouth, and surrounded by extensive mud flats [6]. Figure 1b includes a surveyed cross-section of the sampling site located mi-estuary, in which the vertical elevations are related to the Australian Height Datum (AHD). Figure 1c presents a view of the estuary channel immediately upstream of the sampling site during the early flood tide. Figure 1d shows the probe holding structure at low tide. Table 1 summarises the tidal conditions including the start and end sampling times. Further details on the field investigation were reported in [33].

Turbulent velocities were measured with three acoustic Doppler velocimeters Sontek microADV (16 MHz) located about 10 m from the left bank. Table 2 gives the detailed characteristics of each instrument which was given a four symbol code (e.g. ADV1) used herein to refer to that instrument. Figure 1b shows the location of their sampling volumes in the surveyed experimental cross-section. The velocity measurements were performed continuously at relatively high frequency (50 Hz) for 50 h (Table 1). All the ADV units were synchronised carefully within 20 ms for the entire duration of the study. Note that the ADV2 and ADV3 units were equipped with a 3 component head, while the ADV1 unit had a two component

Table 1 Tidal conditions during the field study at Eprapah Creek QLD, Australia

Date	Time	Tidal height (m AHD)	Sampling rate (Hz)	Remarks
(1)	(2)	(3)	(4)	(5)
6 June 2007	00:54	1.11	50	
	07:21	−0.62		Sampling time start: 08:50
	13:17	0.43		
	19:07	−0.69		
7 June 2007	01:42	1.07		
	08:43	−0.66		
	14:19	0.46		
	20:08	−0.62		
8 June 2007	02:36	1.02		
	09:37	−0.72		Sampling time end: 10:10
	15:29	0.53		
	21:18	−0.57		

Note: Tide times and heights at the river mouth

head (Table 2). The acoustic backscatter intensity of each ADV signal was also analysed. The backscatter intensity is a function of the ADV signal amplitude that is proportional to the number of particles within the sampling volume:

$$I_b = 10^{-5}\, 10^{0.043 Ampl} \quad (1)$$

where the backscatter intensity I_b is dimensionless and the average amplitude Ampl is in counts. (The coefficient 10^{-5} is a value introduced to avoid large values of backscatter intensity.) The backscatter intensity may be used as a proxy for the instantaneous suspended sediment concentration (SSC) because of the strong relationship between I_b and SSC [8,11,30]. Further the term $V_x I_b$ is proportional to the suspended sediment flux per unit area.

A thorough post-processing technique was developed and applied to remove electronic noise, physical disturbances and Doppler effects [7,9]. The field experience demonstrated that the gross ADV signals were unsuitable, and led often to inaccurate time-averaged flow properties. Herein only post-processed data are discussed. Note that the signal processing did not affect the frequency response of the ADVs.

The post-processed data sets included the three instantaneous velocity components V_x, V_y and V_z, and the backscatter intensity I_b, where x is the longitudinal direction positive downstream, y is the transverse direction positive towards the left bank and z is the vertical direction positive upwards. The turbulent fluctuations were defined as : $v = V - \overline{V}$ and $i_b = I_b - \overline{I_b}$, where V was the instantaneous (measured) velocity component, $\overline{V}$ was the variable-interval time average (VITA) velocity and $\overline{I_b}$ is the VITA backscatter intensity. A cut-off frequency was selected with an averaging time greater than the characteristic period of fluctuations, and smaller than the characteristic period for the time-evolution of the mean properties. The selection of the cut-off frequency was derived from a sensitivity analysis [7,34]. Herein all turbulence data, including the turbulent flux events, were processed using samples that contain 10,000 data points (200 s). The turbulence statistics were calculated every 10 s along the entire data sets, although they were not evaluated when more 20% of the 10,000 data points were corrupted/repaired during the ADV data post-processing.

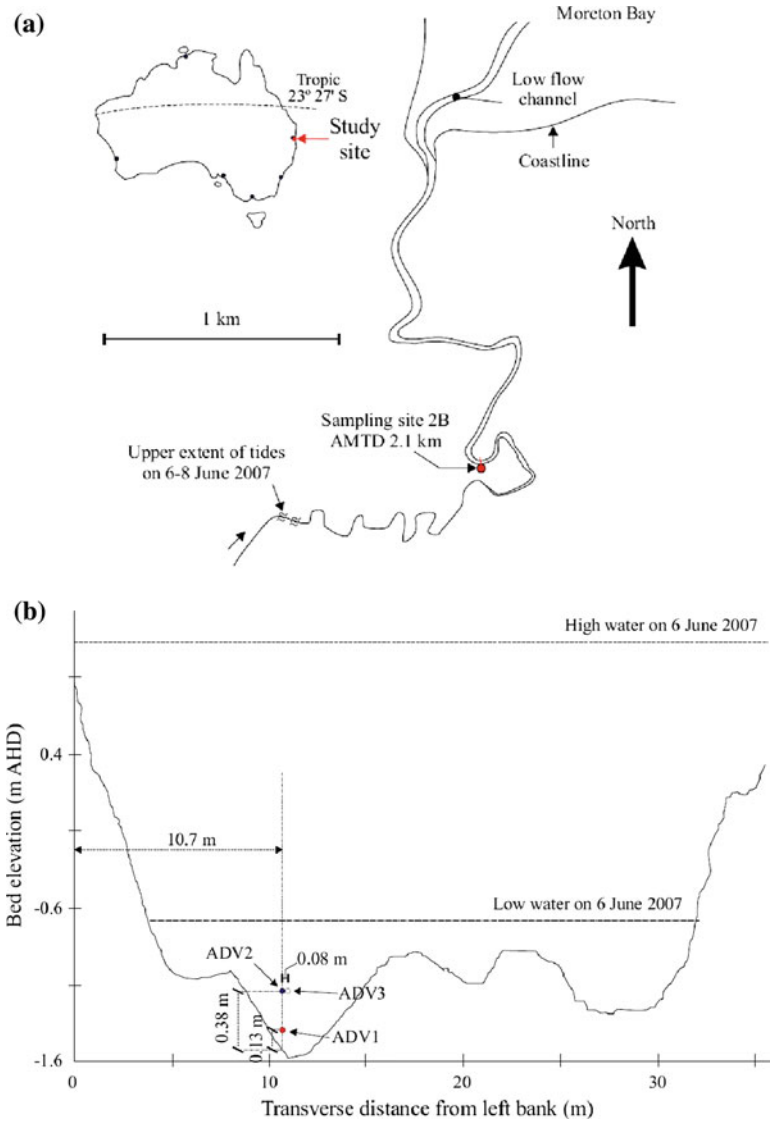

Fig. 1 Investigation site. **a** Map of Eprapah creek estuary; **b** surveyed cross-section, looking downstream; **c** view from the left bank at the sampling site looking upstream on 7 June 2007 at 10:37 ($t = 124,620$ s) during the early flood tide; **d** installation of the tripod supporting the ADVs at low tide on 6 June 2007, viewed from the left bank (Courtesy of Dr S. Furuyama)

3 Turbulent event detection technique

The detection of turbulence bursting events was based upon the technique of Narasimha et al. [18] that was adapted and extended. While this approach differs from more traditional event detection techniques (e.g. [2,13,21]), it was found herein to be a robust method well-suited to the study of the unsteady estuary flow.

Fig. 1 continued

Table 2 Sampling and location information for the ADVs deployed at site 2B, Eprapah Creek on 6–8 June 2007

Instrument code (1)	Instrumentation (2)	Sampling location (3)	f_{scan} (Hz)
ADV1	Sontek 2D-microADV (16 MHz, serial A641F), side-looking head, sampling rate: 50 Hz	AMTD = 2.1 km 0.13 m above bed, 10.7 m from left bank	50
ADV2	Sontek 3D-microADV (16 MHz, serial A813F) down-looking head, sampling rate: 50 Hz	AMTD = 2.1 km 0.38 m above bed, 10.7 m from left bank	50
ADV3	Sontek 3D-microADV (16 MHz, serial A843F) side-looking head, sampling rate: 50 Hz	AMTD = 2.1 km 0.38 m above bed, 10.78 m from left bank	50

Note: AMTD: Adopted middle thread distance measured upstream from river mouth

A turbulent event is basically defined as a series of turbulent fluctuations that contain more energy than the average turbulent fluctuations within a studied data section. The method detects bursting events within a data section by comparing the absolute value of an instantaneous turbulent flux q (e.g. $q = v_x v_z$) with the standard deviation q' of that flux over the data section. That is, a turbulent event occurs if:

$$|q| > k\,q' \tag{2}$$

where $|q|$ is the absolute value of the instantaneous flux q, k is a positive constant setting the threshold and q' is the standard deviation of the quantity q over the data section. Narasimha et al. [18] conducted a sensitivity analysis on the positive multiplier threshold (k). Using data from three different sites, they showed that the total contribution from the events to the total flux remained roughly constant and stays close to 100% for threshold values $k \leq 1$. The threshold value leading to the identification of the smallest number of events that account for all the flux yielded $k = 1$. A similar analysis was conducted herein using 200 s long data sections. The present results yielded good quality results for $k \leq 0.25$ to 0.75. Herein, $k = 1$ was selected to assist with the comparison between estuarine and atmospheric boundary layer data (see below), and consecutive data sections of 10,000 data points (200 s) were used.

For a data section, the information of each detected event was summarised including the event start/finish times, duration τ, dimensionless flux amplitude A and relative magnitude m. The event properties were used to compare individual turbulent events within a data set and between synchronised data sets collected simultaneously. Figure 2a introduces the definition of the duration and amplitude of an isolated event. The duration τ of the event is the time interval between the "zeroes" in momentum flux (e.g. $q = v_x v_z$) nearest to the sequence of data points satisfying Eq. 2. Practically, the event duration is calculated from the first data point with the same sign as the event to the first data point after the change in sign in momentum flux. The present method provides an accurate estimate of the event duration τ within the limitations of the sampling frequency. The dimensionless amplitude A of an event is the ratio of the averaged flux amplitude during the event to the long-term mean flux of the entire data section:

$$A = \frac{1}{\overline{q}} \int_{\tau} q \frac{dt}{\tau} \tag{3}$$

where $\overline{q}$ is the averaged value of q over the data section and $dt = 1/f_{scan}$ ($f_{scan} = 50$ Hz). The relative contribution of an event to the total momentum flux of the data section is called the relative magnitude m defined as:

$$m = \frac{A\,\tau}{T} \tag{4}$$

where T is the total duration of the data section ($T = 200$ s herein). This technique was applied to the momentum fluxes $v_x v_y$ and $v_x v_z$, and to the "pseudo" suspended sediment flux $v_x i_b$, where i_b is the instantaneous fluctuation in the ADV backscatter intensity.

The turbulent event properties may be presented as a time-series of the dimensionless flux amplitude. Such a presentation shows the duration and dimensionless amplitude of each event in a simplified format (e.g. Fig. 3). Figure 3 presents the dimensionless event amplitude of $v_x v_z$ from some data set of the ADV2 and ADV3 units as a function of time for a 10 s sample near the beginning of the study (early flood tide). It is seen that the time series includes both positive and negative amplitude events, each event corresponding to a rectangular pulse. The pulse width is the duration τ and the height is the amplitude A, while the area beneath is proportional to the event magnitude m.

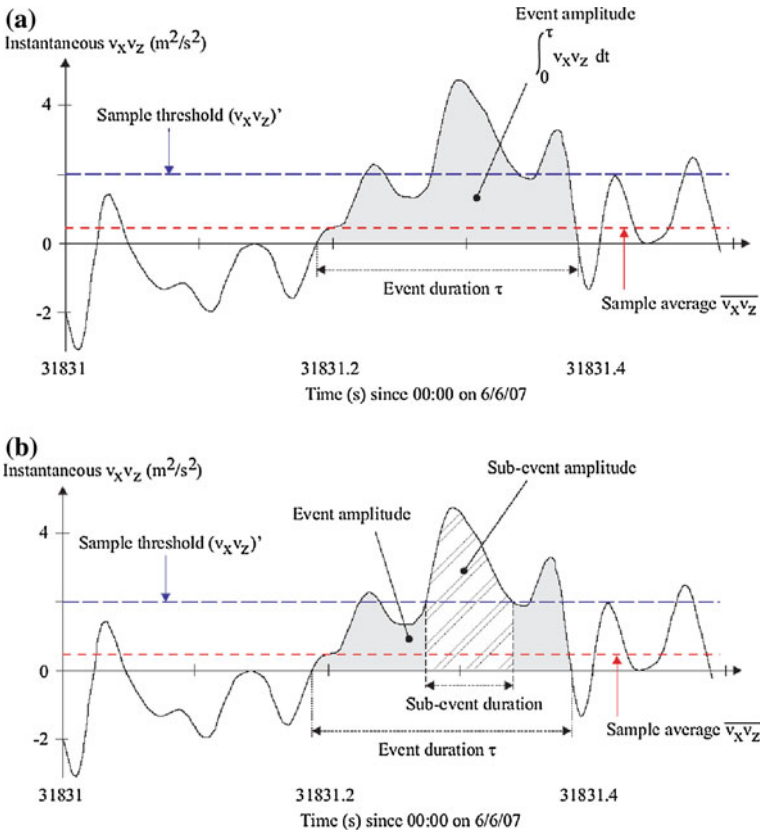

Fig. 2 Turbulent flux event definitions and momentum flux data collected by the ADV2 unit located 0.38 m above bed, approximately 10.7 m from left bank at site 2B, Eprapah creek (6–8 June 2007). **a** Definition sketch of flux event and event parameters; **b** Definition sketch of turbulent sub-events within a turbulent event

3.1 Sub-event analysis

The above method was extended to investigate turbulent sub-events within a large event. For example, in Fig. 2a, the turbulent event is characterised by three distinct peaks in momentum flux and the entire event may be represented as a succession of three consecutive "turbulent sub-events". The second sub-event is sketched in Fig. 2b. Herein a turbulent sub-event was defined when the instantaneous momentum flux within the main turbulent event was greater than the momentum flux threshold (Eq. 2) of the data section. In Fig. 2b, the definition of duration and amplitude of the sub-event are included.

For each sub-event, its start/finish times, duration, dimensionless flux amplitude and relative magnitude were calculated within a given event. The duration of a sub-event is that time interval during which the momentum flux was equal to or greater than the threshold value. For each sub-event, the dimensionless sub-event amplitude is the ratio of the averaged sub-event amplitude to the sub-event duration to the mean flux over the data section. The sub-event properties were calculated for consecutive data sections containing 10,000 data points (200 s) along each data set with the same technique used to analyse turbulence events, including the number of sub-events that occurred in each individual event.

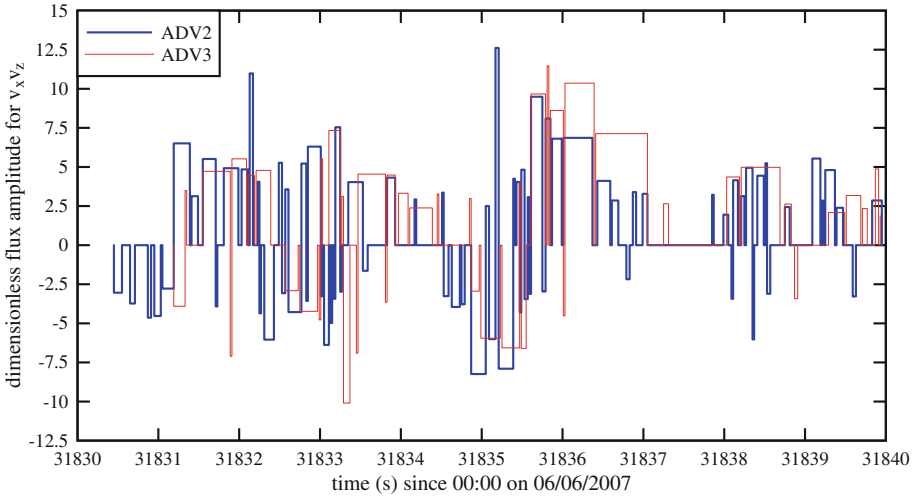

Fig. 3 Dimensionless amplitude of detected turbulent events in terms of $v_x v_z$ for the ADV2 and ADV3 units as functions of time—data collected at site 2B, Eprapah creek for during the study E10 (6–8 June 2007)—ADV2 and ADV3 units located 0.38 m above bed, 10.7 and 10.78 m from left bank respectfully

4 General observations

The field study was conducted on the 6 to 8 June 2007 about mid-estuary (Fig. 1). Figure 1b illustrates the channel cross-section with the respective high and low water levels, and the transverse location of the acoustic Doppler velocimetry (ADV) systems. Although the tides are semi-diurnal, the tidal cycles have slightly different periods and amplitudes indicating that a diurnal inequality exists (Fig. 4). For the entire study, the relative elevation of the sampling volume z/d ranged from 0.15 to 0.53 (average 0.24) for the ADV2 and ADV3 units, where z is the sampling volume elevation above the bed and d is the flow depth. Thus the data were collected in the outer flow region ($z/d > 0.1$) and the data scaling is based upon the outer flow properties.

The time-averaged longitudinal velocity data highlighted the largest ebb and flood velocities occurring around the low tide. For the ADV2 unit ($z = 0.38$ m), Fig. 4 shows the time-averaged longitudinal velocity V_x and the water depth as functions of time, where V_x is positive downstream. The low-pass filtered trend is also included. All the velocity data showed multiple flow reversals around high tides, as well as long-period oscillations. Similar phenomena were observed previously under neap tide conditions at Eprapah Creek [4,32,34]. The multiple flow reversals and low-frequency velocity oscillations had periods between 40 min and 1.5 h, and they were caused by some external resonance in Moreton Bay [34]. Moreton Bay is separated from the Pacific Ocean by three large sand islands. It is approximately 30 km wide North of the Brisbane River and narrows to about 12 km wide near Eprapah Creek, with a mean depth of approximately 5 m, and the dominant resonance periods range from 2,500 s (42 min) to 14,700 s (4 h). The low-pass filtered velocity data showed a slack period ($V_x \approx 0$) at low tide and slightly after high tide (Fig. 4). Although there was no lag between low water (LW) and low water slack (LWS), the time lag between high water (HW) and high water slack (HWS) was about 72 min in average during the study. Such a result is common in convergent estuaries like Eprapah Creek [16,27], and the difference

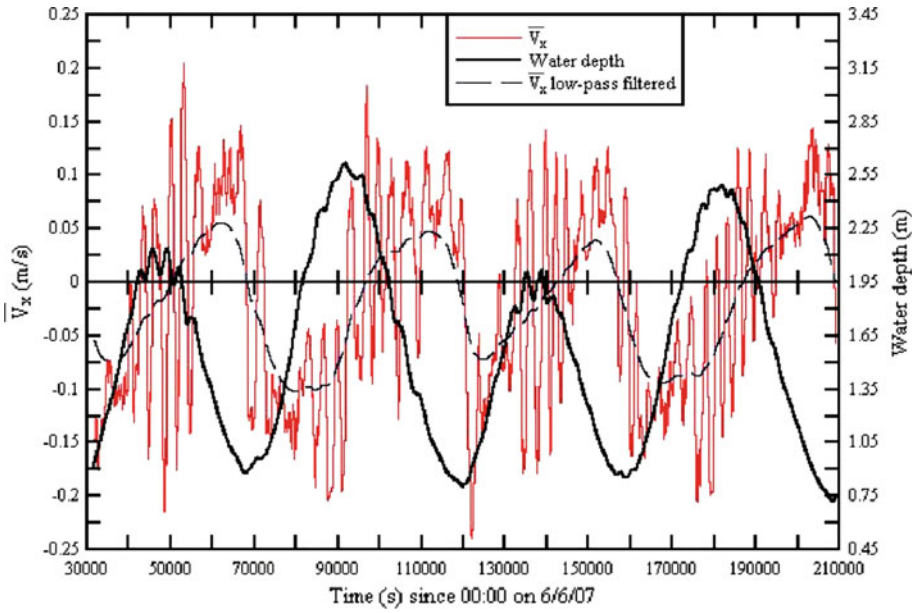

Fig. 4 Time-averaged longitudinal velocity and water depth as functions of time—data collected by the ADV2 unit ($z = 0.38$ m)—VITA calculations using the average of the next 10,000 samples (200 s) at 10 s intervals along entire data sets and low-pass filtered trend (cutoff frequency: 4 10^{-5} Hz)

between LW and HW time lags reflects the large changes in channel cross-sectional area with the water elevation (e.g. Fig. 1b).

The turbulent intensities were large throughout the study. For example, Fig. 5 presents the longitudinal turbulent intensity $v'_x/\overline{V_x}$ for the ADV2 unit located 0.38 m above the bed. At that elevation, the median turbulent intensity was $v'_x/\overline{V_x} = 0.187$. During the field study, the standard deviations of all velocity components and for all units were larger than laboratory data, but a key feature of the natural estuary flow was the significant three-dimensional effects associated with strong secondary currents.

The turbulent Reynolds stresses were calculated for all ADV units [33]. The results showed highly variable near-bed turbulent stresses. Further the Reynolds stress magnitudes varied directly with the magnitude of the longitudinal velocity. They were the largest during the flood tide and during the multiple flow reversals at high tides. For the entire field study, the median tangential Reynolds stresses $\rho\overline{v_x v_z}$ and $\rho\overline{v_x v_y}$ were respectively 0.02 and 0.028 Pa. The present findings were consistent with earlier studies in estuaries (e.g. [29,34]).

5 Turbulent events and sub-events

5.1 Presentation

Traditionally, the Reynolds stress tensor has been used as a descriptor/proxy of the turbulence structure. But a complete characterisation of turbulence encompasses (a) the spatial distribution of Reynolds stresses, and also (b) the rates at which the individual Reynolds stresses are

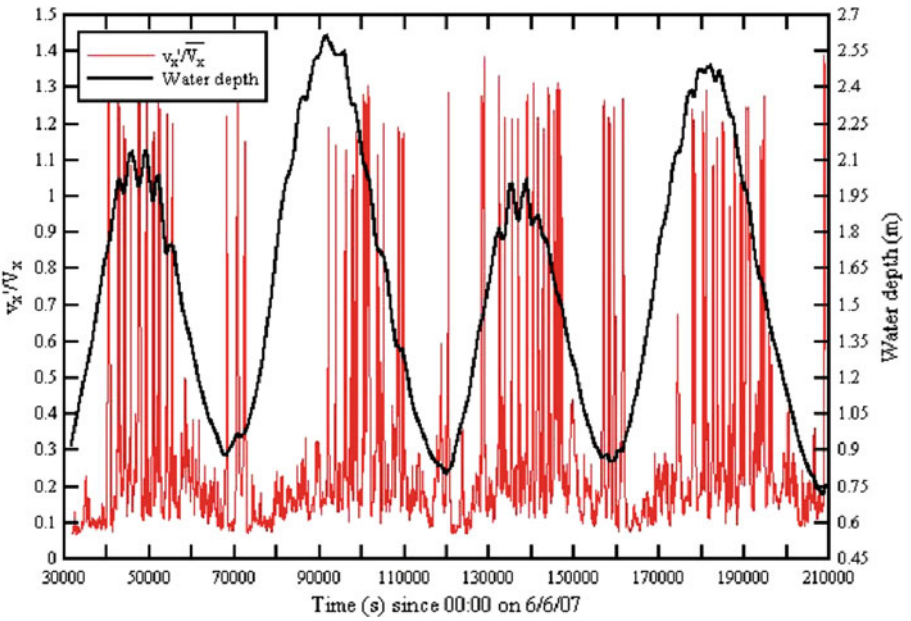

Fig. 5 Dimensionless ratio $v_x'/\overline{V_x}$ as a function of time—data collected by the ADV2 unit ($z = 0.38$ m)

Table 3 Total number of turbulent events and sub-events detected in the ADV data sets for the entire study

ADV unit (1)	Flux (2)	Number of events (3)	Number of sub-events (4)
ADV1	$v_x v_y$	164,706	479,376
	$v_x i_b$	640,046	741,963
ADV2	$v_x v_z$	389,113	712,283
	$v_x v_y$	762,090	982,352
	$v_x i_b$	889,305	743,320
ADV3	$v_x v_z$	542,861	829,317
	$v_x v_y$	242,939	588,094
	$v_x i_b$	885,940	902,951

produced, destroyed or transported from one point in space to another, (c) the contribution of different sizes of eddy to the Reynolds stresses, and (d) the contribution of different sizes of eddy to the rates mentioned in (b) and to rate at which Reynolds stresses are transferred from one range of eddy size to another ([3]). It is argued herein that a turbulent event analysis is a simpler approach, as demonstrated by seminal turbulence studies including [1,2,13,17,19] and [21].

Turbulent events and sub-events were investigated for the turbulent fluxes $v_x v_z$, $v_x v_y$, and $v_x i_b$, using the data collected by the ADV1, ADV2 and ADV3 units. Table 3 summarises the number of events and sub-events detected in the ADV data sets collected for the entire study. For the whole data set, the histograms of event duration, event amplitude, sub-event duration and sub-event amplitude were calculated. Figure 6 shows the normalised probability density functions of event duration τ for the momentum fluxes $v_x v_z$, $v_x v_y$, and $v_x i_b$, while Fig. 7

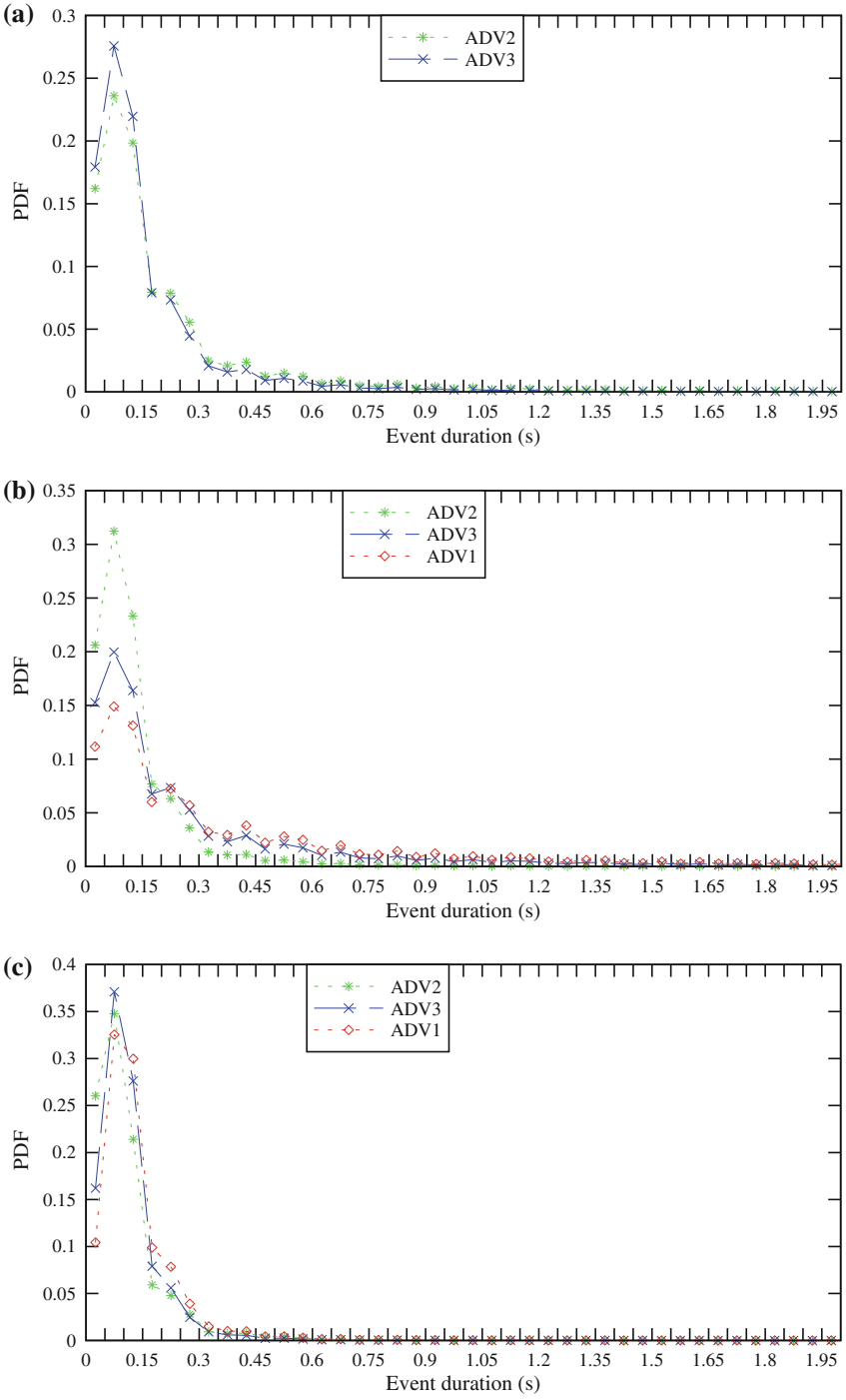

Fig. 6 Normalised probability density functions of event duration for the momentum fluxes $v_x v_z$, $v_x v_y$ and $v_x i_b$—data collected by the ADV1, ADV2 and ADV3 units—event duration histogram intervals = 0.05 s. **a** Event duration for $v_x v_z$; **b** event duration for $v_x v_y$; **c** event duration for $v_x i_b$

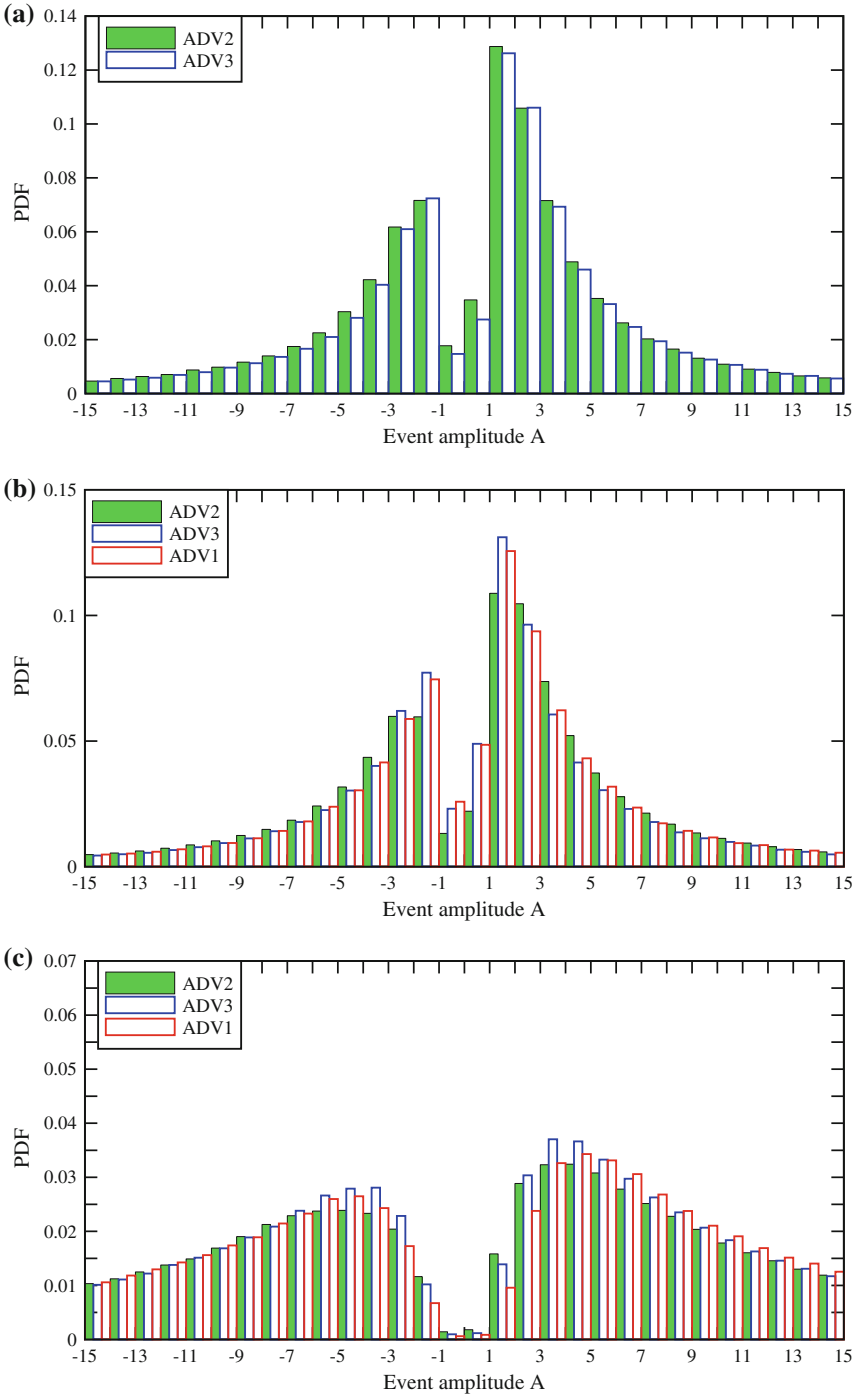

Fig. 7 Normalised probability density functions of dimensionless amplitude for the momentum fluxes $v_x v_z$, $v_x v_y$ and $v_x i_b$—data collected by the ADV1, ADV2 and ADV3 units—event amplitude histogram interval = 1. **a** Event amplitude for $v_x v_z$; **b** event amplitude for $v_x v_y$; **c** event amplitude for $v_x i_b$

presents the normalised probability density functions of the corresponding dimensionless event amplitude A. The statistical properties of turbulent event durations, amplitudes and magnitudes are summarised in Tables 4 and 5.

During the field study, the majority of turbulent events had a duration between $0.08 < \tau < 0.3$ s (0.2 s on average) for all momentum fluxes (Fig. 6). The probability distributions functions of event durations presented a skewed shape (Fig. 6) in qualitative agreement with turbulent boundary layer measurements [1] and dye concentration measurements in open channel [23]. On average, the dimensionless event duration was about $\tau\,\overline{|V_x|}/d = 0.07$ with $\overline{|V_x|}$ the average magnitude of longitudinal velocity component. For comparison, laboratory data in developing boundary layers yielded dimensionless event durations between 0.2 and 0.6 [1,17], while dimensionless dye concentration burst durations between 0.06 and 0.07 were reported in a laboratory open flume [23].

The distributions of event amplitude included the information on the type of event: positive or negative (Fig. 7). For a steady ebb tide flow ($\overline{V_x} > 0$), ejections and sweeps (quadrant Q2 or Q4) would correspond to a negative event amplitude for the momentum flux $q = v_x v_z$, while a positive amplitude implied a wallward or outward interaction (quadrant Q1 or Q3). For an unsteady estuary flow, the physical interpretation of an event type was more complicated because of the changes in flow direction and in sign of time-averaged flux over a data section (see below). The data presented a similar shape for the fluxes $v_x v_z$ and $v_x v_y$ (Fig. 7). For the entire study and all fluxes, the median amplitude modulus was between $3 \leq |A| \leq 14$. For each turbulent flux, the event amplitude distribution tended to indicate a larger proportion of positive events than of negative events for all ADV units. Next to a boundary, the turbulent bursting process is composed of a quasi-periodic cycle of ejections and sweep motions (e.g. [19,22]). The present data sets suggested comparatively a large number of negative events than of positive events. However, for all the fluxes, the positive events ($A > 0$) were on average longer and of smaller amplitude than the negative events, with a similar event magnitude overall (Table 4). Table 4 summarises the median values of number of events per sample, event duration, dimensionless event amplitude, and relative event magnitude for each ADV unit. Although there were some differences between the three velocimeters (Tables 4 and 5), the statistical results were relatively close and tended to show little effect of the sampling volume location.

5.2 Turbulence event statistics

The turbulent event statistics were collected over a 200 s sample (10,000 data points) every 10 s along the entire ADV data sets. The event statistics were sampled in a similar fashion to all turbulence properties, thereby allowing for observations of any tidal trend. Figure 8 presents the time-variation of the number of events per sample, the median event duration and the median event amplitude for the momentum flux $v_x v_z$ of the ADV2 unit.

For the entire study, there were on average $n = 1$ to 4 turbulent events per seconds for all the fluxes (Table 4), and the result was close for all ADV units. The dimensionless event rate $n\,d/\overline{|V_x|}$ ranged from 22 to 88, somehow larger than earlier laboratory data $n\,d/\overline{|V_x|} = 1.8$ to 8 obtained with different instrumentations and event detection techniques [13,15,25]. For all momentum fluxes and all ADV units, the number of events per sample varied in a similar pattern with the tides (Fig. 8a). The turbulent event rate n increased about low tide when the water column was shallower, the effects of bed shear stress were stronger and the depth-averaged velocity gradient was the largest. Conversely, the event rate decreased about high tide.

Table 4 Basic turbulent event characteristics for the ADV1, ADV2 and ADV3 units during the entire field study

Parameter	ADV1 unit		ADV2 unit			ADV3 unit		
(1)	$v_x v_y$ (2)	$v_x i_b$ (3)	$v_x v_z$ (4)	$v_x v_y$ (5)	$v_x i_b$ (6)	$v_x v_z$ (7)	$v_x v_y$ (8)	$v_x i_b$ (9)
Nb of events per data sample	154	743	389	912	988	614	221	1,050
Event duration τ (*s*)								
Median duration of positive events ($A > 0$) (s)	0.26	0.10	0.12	0.10	0.08	0.10	0.16	0.40
Median duration of negative events ($A < 0$) (s)	0.18	0.10	0.10	0.08	0.06	0.08	0.12	0.08
Event amplitude A								
Median amplitude of positive events ($A > 0$)	3.34	11.87	3.44	3.87	11.9	3.56	3.26	11.04
Median amplitude of negative events ($A < 0$)	−4.21	−13.34	−4.06	−4.67	−13.3	−4.31	−4.08	−12.19
Relative magnitude m								
Median magnitude of positive events ($A < 0$)	0.0048	0.0069	0.0026	0.0021	0.0055	0.0023	0.0033	0.0055
Median magnitude of negative events ($A < 0$)	−0.0045	−0.0067	−0.0023	−0.0020	−0.0052	−0.0023	−0.0030	−0.0053

Note: data sample length = 200 s (10,000 data points)

Table 5 Statistical properties of turbulent event duration, amplitude and magnitude for the ADV1, ADV2 and ADV3 units during the entire field study

Parameter	ADV1 unit		ADV2 unit			ADV3 unit		
(1)	$v_x v_y$ (2)	$v_x i_b$ (3)	$v_x v_z$ (4)	$v_x v_y$ (5)	$v_x i_b$ (6)	$v_x v_z$ (7)	$v_x v_y$ (8)	$v_x i_b$ (9)
Median event duration τ (s)	0.38	0.1	0.16	0.08	0.08	0.1	0.24	0.08
Standard deviation (s)	4.49	0.04	0.42	0.05	0.06	0.08	3.71	0.04
Skewness	18.39	12.55	21.80	3.67	17.09	2.65	15.90	17.62
Kurtosis	427.7	419.5	1,002.3	23.6	331.5	13.9	301.8	422.4
Median event amplitude A	1.335	4.21	1.38	1.85	3.17	1.61	1.31	4.05
Standard deviation	7,333	1,183	508	163	2,449	208	285	3,341
Skewness	131	71	122	-69	121	62	71	128
Kurtosis	17,049	5,633	15,556	6,335	15,621	5,748	9,210	16,673
Median event magnitude m	0.0012	0.0016	0.0009	0.0007	0.0011	0.0007	0.0009	0.0014
Standard deviation	5.18	0.44	0.44	0.05	0.70	0.07	0.12	1.24
Skewness	130.6	–5.7	129.8	–64.3	–123.3	61.2	38.5	128.7
Kurtosis	17,060	4,801	16,976	5,795	15,815	5,311	3,612	16,733

Note: data sample length = 200 s (10,000 data points)

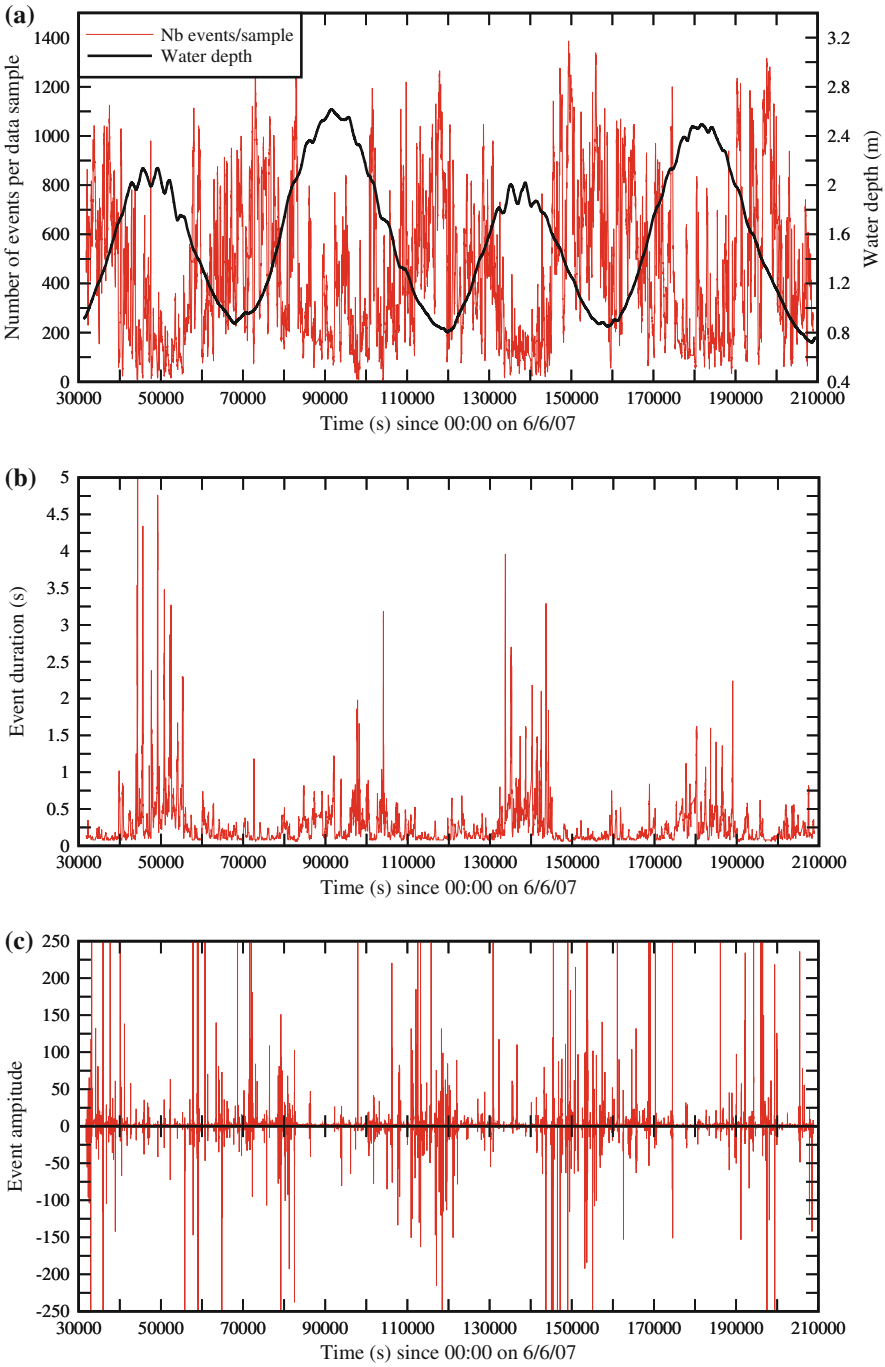

Fig. 8 Time variations of the median event duration and amplitude, and number of events per sample for $v_x v_z$ during the entire study—data collected by the ADV2 unit ($z = 0.38$ m)—calculations conducted over 10,000 data points (200 s) every 10 s along entire data sets (VITA calculations using the average of the next 10,000 samples). **a** Number of events per sample; **b** event duration τ (s); **c** event amplitude A

Table 6 Median sub-event characteristics for the ADV1, ADV2 and ADV3 units during the entire field study

Parameter	ADV1 unit		ADV2 unit			ADV3 unit		
(1)	$v_x v_y$ (2)	$v_x i_b$ (3)	$v_x v_z$ (4)	$v_x v_y$ (5)	$v_x i_b$ (6)	$v_x v_z$ (7)	$v_x v_y$ (8)	$v_x i_b$ (9)
Nb of sub-events per data sample	540	982	910	1,375	1,195	1,107	707	1,284
Sub-event duration (s)								
Median duration of positive sub-events ($A > 0$) (s)	0.04	0.04	0.04	0.04	0.04	0.04	0.04	0.04
Median duration of negative sub-events ($A < 0$) (s)	0.04	0.04	0.04	0.04	0.04	0.04	0.04	0.04
Sub-event amplitude A								
Median amplitude of positive sub-events ($A > 0$)	2.83	12.67	3.18	4.09	11.81	3.57	2.76	11.55
Median amplitude of negative sub-events ($A < 0$)	–5.28	–15.98	–4.84	–6.37	–15.38	–5.41	–5.08	–14.65
Sub-event magnitude m								
Median magnitude of positive sub-events ($A > 0$)	0.0009	0.0033	0.0009	0.0010	0.0029	0.0010	0.0008	0.0029
Median magnitude of negative sub-events ($A < 0$)	–0.0014	–0.0038	–0.0012	–0.0015	–0.0035	–0.0013	–0.0013	–0.0034

Note: data sample length = 200 s (10,000 data points)

The event duration for the momentum fluxes $v_x v_z$ and $v_x v_y$ seemed to vary with the tides for all the ADV systems (Fig. 8b), while the pseudo suspended sediment flux event duration data $v_x i_b$ showed no discernable tidal pattern. In Fig. 8b, the event duration of $v_x v_z$ for the ADV2 unit was the largest about the high tides and smallest about the low tides. A similar tidal pattern was observed for the event durations of $v_x v_z$ with the ADV3 unit, and for event duration of $v_x v_y$ for all ADV units. Figure 8c shows that the event amplitude of $v_x v_z$ for the ADV2 unit varied with the tides, with the magnitude of event amplitude being larger about low water and smaller about high water. No discernable tidal patterns in terms of event amplitude of $v_x v_y$ and $v_x i_b$ fluxes were observed for all ADV units.

5.3 Turbulence sub-event statistics

Turbulent sub-events were investigated in terms of the fluxes $v_x v_z$, $v_x v_y$ and $v_x i_b$, using the data collected by the three ADV units. Table 6 summarises the median values of the number of sub-events per sample, the sub-event duration, dimensionless sub-event amplitude, and the relative sub-event magnitude. The median sub-event duration was 0.04 s for all fluxes and ADV units, implying that most sub-events had a short life span. The sub-event amplitudes for the fluxes $v_x v_z$ and $v_x v_y$ were typically between 2.8 and 6.4. For comparison, the sub-event amplitudes for the suspended sediment flux $v_x i_b$ were larger, between 11 and 16 (Table 6).

The present data highlighted first that the definition of a large turbulent event is not straightforward. A large turbulent burst may in fact be the cumulative effect of smaller events, called sub-events (Fig. 2). Herein the sub-events were major episodes of amplitude comparable to

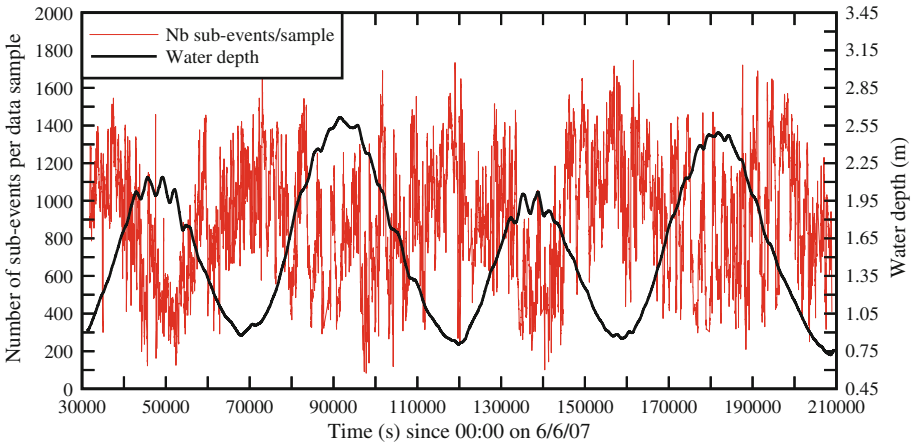

Fig. 9 Time-variation of the number of sub-events per sample for the momentum flux $v_x v_z$—data collected by the ADV2 unit ($z = 0.38$ m)—calculations conducted over 10,000 data points (200 s) every 10 s along the entire data set

main turbulent event amplitudes (Tables 4 and 6). Their existence may derive from the vortex pairing of large-scale bursts produced in the inner region of the flow, close to the bed, and advected into the outer flow region where the measurements were taken, as proposed by [1].

Figure 9 illustrates the time-variation of the number of sub-events per data sample ($T = 200$ s) for the momentum flux $v_x v_z$ at $z = 0.38$ m. For all fluxes and all ADV units, the number of sub-events per sample varied in a similar fashion with the tides (Fig. 9). That is, it increased about low tide and decreased about high tide. Basically the number of turbulent sub-events per sample increased about low tide when the water column was shallower because of the stronger influence of bed shear stress on the water column. Altogether the time-variation of the number of sub-events per sample exhibited a similar tidal pattern to that of the number of events per sample (Fig. 8a).

For the entire field study, the events durations showed no obvious tidal trend while, for the sub-event amplitude, only those of the momentum flux $v_x v_z$ seemed to vary with the tide. Herein the sub-event amplitude of the flux $v_x v_z$ showed a similar tidal trend to that of the event amplitude for $v_x v_z$, being largest about low tide and smallest about high tide. On average over the entire study, the results showed 1 to 3 sub-events per turbulent event and the finding was independent of the tidal period (Table 3).

6 Discussion

6.1 Comparison between estuarine and atmospheric boundary layer data

The present findings in an estuary may be compared with the field data of [26] in an atmospheric boundary layer, re-analysed by [18]. That study was based upon data collected at Jodhpur with an acoustic anemometer located at 4 m above the ground. Table 7 compares the sampling techniques and conditions. The comparative results are presented herein in terms of the momentum flux events for $v_x v_z$ and the basic results are summarised in Table 8.

The results (Table 8) showed that the durations of the events were of the order of 0.11 and 1.4 s respectively for the estuary and atmospheric studies, compared to an outer time scale of

Table 7 Basic data on test sites and flow conditions for turbulent flux event analysis

Parameters	Present study		Rudra Kumar et al. [26]
	ADV1 unit	ADV2 unit	Jodhpur, India
(1)	(2)	(3)	(4)
Fluid:	Brackish water	Brackish water	Air
Instrumentation:	MicroADV (16 MHz)	MicroADV (16 MHz)	Sonic anemometer
Sampling rate (Hz):	50	50	8.41
z (m) =	0.13	0.38	4
z/d, z/δ =	z/d = 0.06 (low tide)	z/d = 0.15 (low tide)	z/δ $\approx$0.01
	z/d = 0.18 (high tide)	z/d = 0.53 (high tide)	
Average velocity magnitude $\lvert V_x \rvert$ (m/s) =	0.061	0.0805	3.15
Average shear velocity V_* (m/s) =	0.0023	0.0023	0.437
$Re_z = \rho \lvert V_x \rvert z/\mu$ =	7.9×10^3	3.0×10^4	8.4×10^5

Table 8 Momentum flux event analyses in terms of $v_x v_z$: comparative results

Parameters	Present study ADV2 unit	Narasimha et al. (2007) Jodhpur, India
(1)	(2)	(3)
z(m) =	0.38	4
Mean momentum flux (m^2/s^2):	2.1×10^{-5}	0.191
Ratio r.m.s/mean :	2.98	3.04
Sweep ejection period:	40%	36%
Wallward/inward interaction period:	16.6%	15%
Idle/passive period	43.4%	49%
Average duration of positive events n_+ ($A > 0$) (s):	0.12	1.71
Average duration of negative events n_- ($A < 0$) (s):	0.10	1.12
Outer time scale (s):	$\sim$15 (mode)	$\sim$30
Burstiness index B =	0.85	0.72

the order of 15 and 30 s respectively. In the present study, the outer time scale was based upon the measured water depth and the velocity magnitude recorded at $z = 0.38$ m since there was no velocity meter closer to the free-surface. Hence the outer time scale estimate was a very rough average and could vary over a wide range from as low as 3 to over 100 s. Overall the differences between turbulent event durations and outer time scales were comparable for both environmental flow studies.

The burstiness index (B) was calculated using the same method as [18] (Table 8). The burstiness index ranges from 0 to 1 and characterises a fractional contribution of the bursting events. In an estuary, the present results gave $B = 0.85$ compared to $B = 0.72$ in atmospheric boundary layers. This suggested a greater contribution of the turbulent events in terms of the momentum flux $v_x v_z$ in the estuary, possibly caused by the secondary flow motion in the confined river channel.

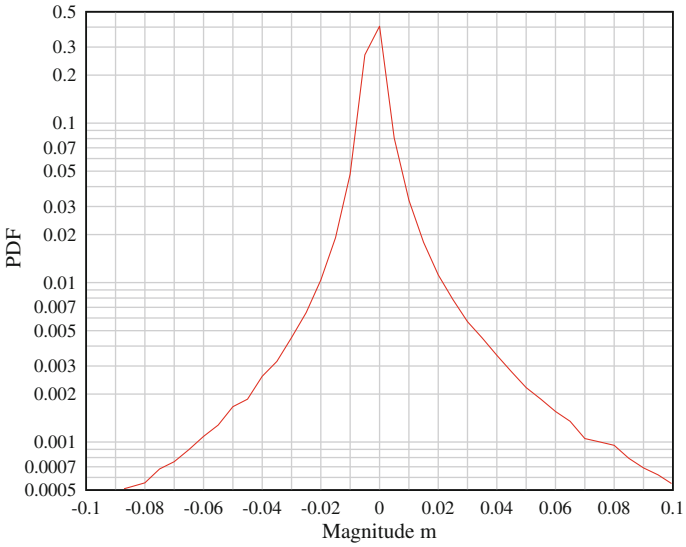

Fig. 10 Normalised probability density function of dimensionless event magnitude m for the momentum flux $v_x v_z$—data collected by the ADV2 unit ($z = 0.38$ m) for the entire study—event magnitude histogram interval = 0.005

Figures 6a, 7a and 10 present the dimensionless probability density functions (PDFs) of the momentum flux $v_x v_z$ for the entire field study. The results may be compared with the corresponding data of ([18], Fig. 6), although the results of Narasimha et al. corresponded a much shorter data set (10 min). The PDF of event duration tended to follow a log-normal distribution for both studies (Fig. 6a). While a log-normal PDF implies that the process is the multiplicative product of a large number of independent, identically-distributed variables, the implications in terms of turbulent event duration remain unclear. But the PDF of event magnitude presented some marked difference with the atmospheric flow results of [18], with a much narrower event magnitude distribution, as well as a different PDF shape, in the present data set (Fig. 10).

The data suggested nil correlation between a turbulent event amplitude and its duration. This is illustrated in Fig. 11 presenting the relationship between turbulent event amplitude A and event duration τ. Figure 11a shows A as function of τ and it may be compared with Fig. 7 of [18]. Figure 11b presents the variations in standard deviations and skewness of |A| with τ, for the data plotted in Fig. 11a. The present data illustrated negligible correlation between the event amplitude and the event duration, and the fluctuations in |A| were independent of the the event duration. The finding was found independently of the tidal phase. Simply, there were a wide range of event amplitudes for any given event duration (Fig. 11b), and conversely. The finding was valid for both geophysical studies (Table 7) and implied that the size of an event and its duration may be considered as two independent parameters.

For all fluxes and ADV units, the PDFs of the number of turbulent sub-events per burst events were skewed with a very large proportion of events having between 1 and 2 sub-events. The PDFs had however a long tail of small numbers of turbulent events with large numbers of sub-events. This is illustrated in Fig. 12 presenting the normalised PDF for the number of sub-events per events for all fluxes at $z = 0.38$ m For the momentum flux $v_x v_z$, the average number of sub-events per event was 1.21 for that data set, and the maximum number of

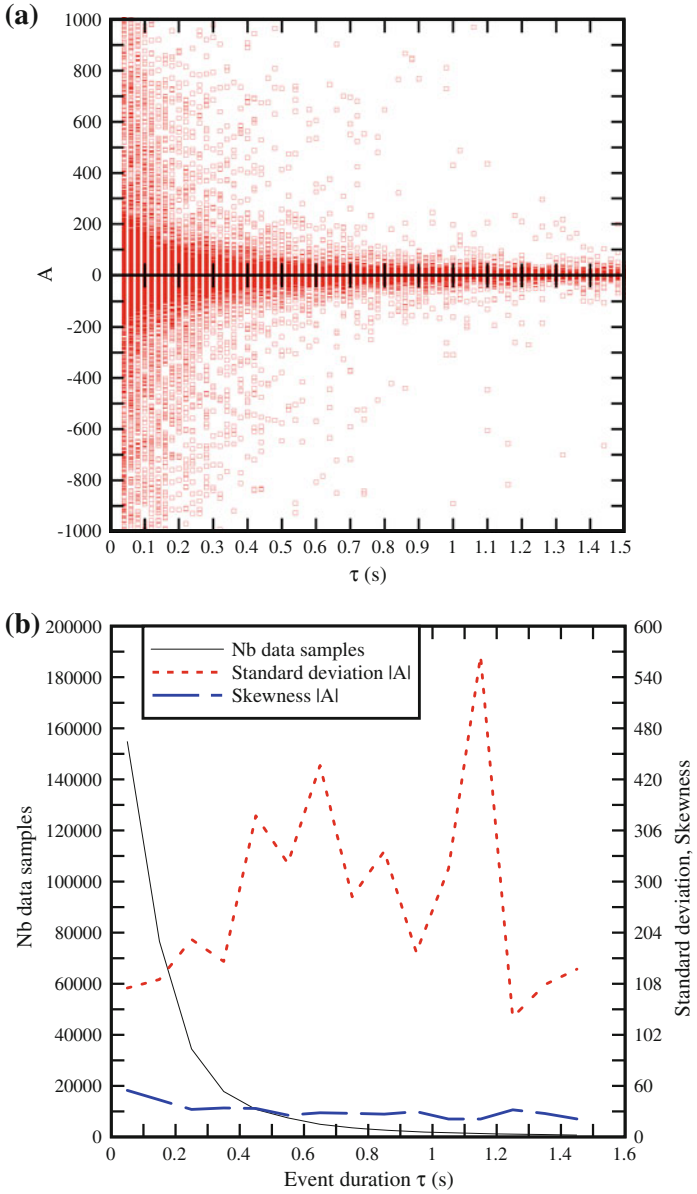

Fig. 11 Relationship between event amplitude A and event duration τ for the momentum flux $v_x v_z$—data collected by the ADV2 unit ($z = 0.38$ m) for the entire study. **a** Event amplitude A as a function of the event duration τ; **b** Standard deviation and skewness of |A| as a function of τ—the number of data samples of each category is also shown

sub-events per event was 440, with 5,420 turbulent events having 40 sub-events or more for the entire study. Overall the distribution of "extreme" numbers of sub-events per turbulent events showed no tidal trend, nor correlation with the longitudinal velocity V_x.

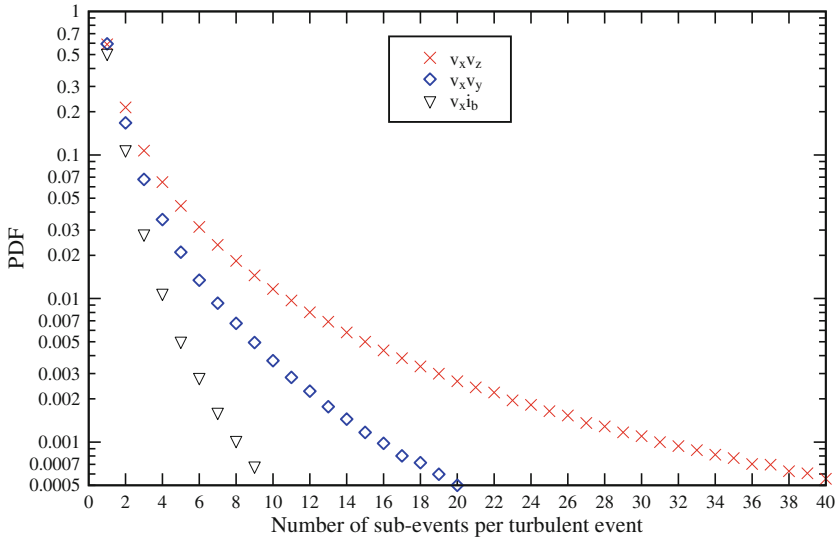

Fig. 12 Normalised probability density function of the number of turbulent sub-events per turbulent event for the momentum flux $v_x v_z$, $v_x v_y$ and $v_x i_b$—data collected by the ADV2 unit ($z = 0.38$ m) for the entire study

6.2 Definition of positive and negative events in unsteady flows

The concept of positive and negative turbulent events was originally based upon the sign of the amplitude A. Considering a quasi-steady flow ($\overline{V_x} > 0$), for the momentum flux $q = v_x v_z$, the ejections ($v_x < 0, v_z > 0$) and sweeps ($v_x > 0, v_z < 0$) were associated with a negative event amplitude, while a positive amplitude implied a wallward or outward interaction. The definition (Eq. 3) was developed for quasi-stationary boundary layer flows and applied to data sets with positive longitudinal velocity ($\overline{V_x} > 0$) and constant sign time-averaged fluxes ($\overline{q}$) by [18].

In estuaries, however, the flow direction changed several times during a complete tidal cycle (e.g. Fig. 4) and similarly the sign of time-averaged fluxes. Furthermore, during some data sections ($T = 200$ s), the time-averaged flux term ($\overline{q}$) might be negligible, close to zero, yielding meaningless physical interpretation of the amplitude sign. In other words, the interpretation of Eq. 3 has some limitations in unsteady geophysical flows.

A modification of Eq. 3 was tested:

$$A = \frac{1}{|\overline{q}|} \int_{\tau} q \frac{dt}{\tau} \tag{5}$$

using the absolute value of flux data section average ($|\overline{q}|$). The impact of the event amplitude definition (Eq. 5 was tested over the entire data sets. The comparative results demonstrated conclusively that the definition of event amplitude had a major impact on the results. Typical results are presented in Fig. 13 in terms of the event magnitude for the momentum flux $q = v_x v_z$. Figure 13a is comparable to Fig. 7a, while Fig. 13b may be compared to Fig. 11a (also Fig. 7 in [18]).

In complex geophysical flows, including estuarine hydrodynamics, a newer event amplitude definition must be introduced to take into account the physical processes. While Eq. 5

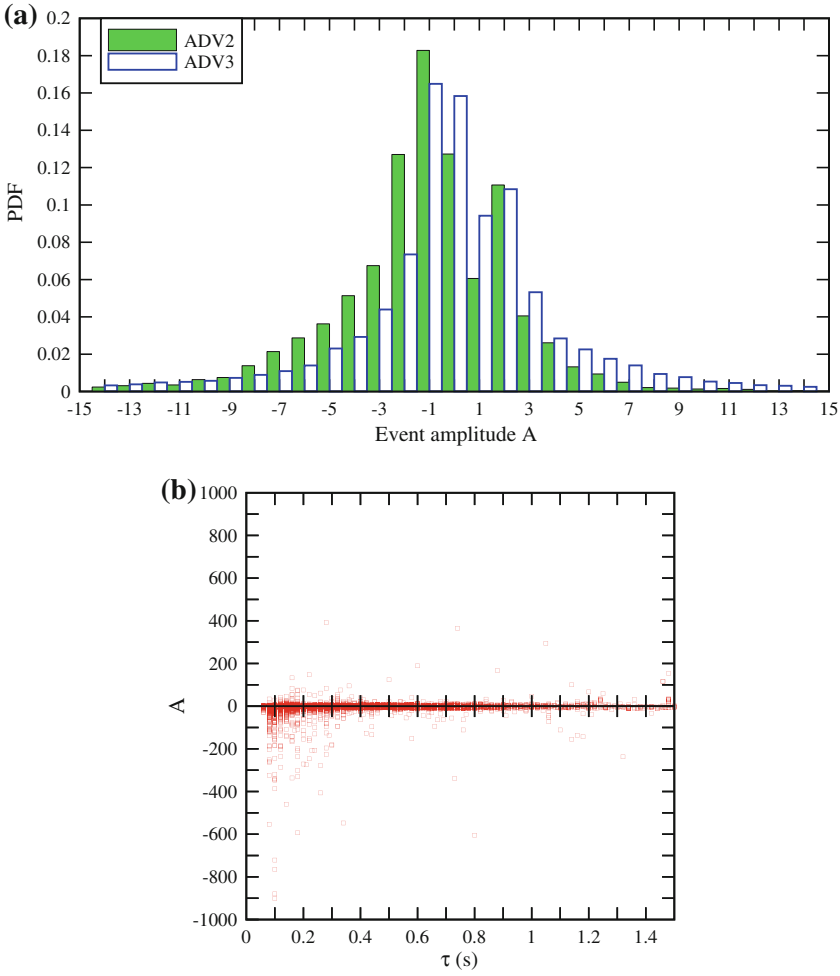

Fig. 13 Effects of the turbulent event amplitude definition on the event amplitude data: application of Eq. 5 to estuarine data. **a** Normalised probability density functions of dimensionless event amplitude for the momentum fluxes $v_x v_z$ using Eq. 5—data collected by the ADV2 and ADV3 units—event amplitude histogram interval = 1; **b** Event amplitude A as a function of the event duration τ for the momentum flux $v_x v_z$ using Eq. 5—data collected by the ADV2 unit ($z = 0.38$ m) for the entire study

might be simplistic, it could be more appropriate in these flows than Eq. 3 developed for quasi-stationary boundary layer flows.

7 Conclusion

Detailed turbulence field measurements were conducted in a small subtropical estuary with semi-diurnal tides under neap tide conditions. Acoustic Doppler velocimetry was used at fixed locations, and sampled continuously for 50 h. A turbulent flux event analysis was performed for the entire data sets. While the Reynolds stresses were used to describe the turbulence structure in past estuarine studies, it is proposed herein that a turbulent event analysis is a simpler approach, as demonstrated by seminal turbulence studies ([1,13]). Following the

technique of [18], turbulent bursting events were defined in terms of the instantaneous turbulent flux. The method was extended to the unsteady estuarine flow motion, and it included some sub-event analyses and some pseudo-sediment flux event calculations.

The turbulent event data showed close results between all three ADV units and all fluxes. The very-large majority of turbulent events had a duration between 0.04 and 0.3 s, and there were on average 1 to 4 turbulent events per second. A number of turbulent bursting event consisted of consecutive turbulent sub-events, with between 1 and 3 sub-events per event on average for all turbulent fluxes. For all ADV systems, the number of events, event duration and event amplitude showed some tidal trends, with key differences between high- and low-water periods.

A comparison between the present estuary data and the atmospheric boundary layer results of [18] illustrated a number of similarities between the two turbulent flows. Both studies implied that the amplitude of an event and its duration were nearly two independent parameters. The data analyses demonstrated the significance of turbulent events in environmental flows, documented their characteristics in an unsteady estuarine channel and showed the complex nature of bursting events consisting of consecutive sub-events. Altogether the present work suggested that the turbulent event analysis is a relatively simple approach and it provides some details into the turbulent bursts that are responsible for major mixing and sedimentary processes. The detailed field measurements highlighted also the large fluctuations in all turbulence characteristics during the tidal cycle.

Acknowledgments The writers acknowledge the support of and input from Dr Richard Brown (Q.U.T.). They thank all the people who participated to the field works.

References

1. Antonia RA (1972) Conditionally sampled measurements near the outer edge of a turbulent boundary layer. J Fluid Mech 56(Part 1):1–18. doi:10.1017/S0022112072002149
2. Bauer BO, Yi J, Namikas SL, Sherman DJ (1998) Event detection and conditional averaging in unsteady Aeolian systems. J Arid Environ 39:345–375. doi:10.1006/jare.1998.0380
3. Bradshaw P (1971) An introduction to turbulence and its measurement. Pergamon Press, Oxford, UK, The Commonwealth and International Library of Science and technology Engineering and Liberal Studies, Thermodynamics and Fluid Mechanics Division, 218 pp
4. Chanson H (2003) A hydraulic, environmental and ecological assessment of a sub-tropical stream in eastern Australia: Eprapah Creek, Victoria Point QLD on 4 April 2003. Report No. CH52/03, Dept. of Civil Engineering, The University of Queensland, Brisbane, Australia, June, 189pp
5. Chanson H (2004) Environmental hydraulics of open channel flows. Elsevier Butterworth-Heinemann, Oxford, UK, 483 pp
6. Chanson H, Brown R, Ferris J, Ramsay I, Warburton K (2005) Preliminary measurements of turbulence and environmental parameters in a sub-tropical estuary of eastern Australia. Environ Fluid Mech 5(6):553–575. doi:10.1007/s10652-005-0928-y
7. Chanson H, Trevethan M, Aoki S (2005) Acoustic Doppler Velocimetry (ADV) in a small estuarine system. Field experience and despiking. In: Jun BH, Lee SI, Seo IW, Choi GW (eds) Proceedings of the 31st Biennial IAHR Congress, Seoul, Korea, Theme E2, Paper 0161, pp 3954–3966
8. Chanson H, Takeuchi M, Trevethan M (2008) Using turbidity and acoustic backscatter intensity as surrogate measures of suspended sediment concentration in a small sub-tropical estuary. J Environ Manag 88(4):1406–1416. doi:10.1016/j.jenvman.2007.07.009
9. Chanson H, Trevethan M, Aoki S (2008) Acoustic Doppler Velocimetry (ADV) in small estuary: field experience and signal post-processing. Flow Meas Instrum 19(5):307–313. doi:10.1016/j.flowmeasinst.2008.03.003
10. Finnigan J (2000) Turbulence in plant canopies. Annu Rev Fluid Mech 32:519–571. doi:10.1146/annurev.fluid.32.1.519
11. Fugate DC, Friedrichs CT (2002) Determining concentration and fall velocity of estuarine particle populations using ADV, OBS and LISST. Cont Shelf Res 22:1867–1886. doi:10.1016/S0278-4343(02)00043-2

12. van der Ham R, Fromtijn HL, Kranenburg C, Winterwerp JC (2001) Turbulent exchange of fine sediments in a tidal channel in the Ems/Dollard estuary. Part I: turbulence measurements. Cont Shelf Res 21:1605–1628. doi:10.1016/S0278-4343(01)00010-3
13. Johansson AV, Alfredsson PH (1982) On the structure of turbulent channel flow. J Fluid Mech 122:295–314. doi:10.1017/S0022112082002225
14. Kawanisi K, Yokosi S (1994) Mean and turbulence characteristics in a tidal river. Cont Shelf Res 17(8):859–875. doi:10.1016/S0278-4343(96)00066-0
15. Kline SJ, Reynolds WC, Schraub FA, Runstaller PW (1967) The structure of turbulent boundary layers. J Fluid Mech 30(4):741–773. doi:10.1017/S0022112067001740
16. Lanzoni S, Seminara G (1998) On tide propagation in convergent estuaries. J Geophys Res. AGU 103(C13):30793–30812
17. Nakagawa H, Nezu I (1981) Structure of space–time correlations of bursting phenomena in an open channel flow. J Fluid Mech 104:1–43. doi:10.1017/S0022112081002796
18. Narasimha R, Rudra Kumar S, Prabhu A, Kailas SV (2007) Turbulent flux events in a nearly neutral atmospheric boundary layer. Phil Trans R Soc Ser A 365:841–858. doi:10.1098/rsta.2006.1949
19. Nezu I, Nakagawa H (1993) Turbulence in open-channel flows. IAHR Monograph, IAHR Fluid Mechanics Section, Balkema Publ., Rotterdam, The Netherlands, 281 pp
20. Nielsen P (1992) Coastal bottom boundary layers and sediment transport. Advanced series on ocean engineering, vol 4. World Scientific Publishers, Singapore
21. Osterlund JM, Lindgren B, Johansson AV (2003) Flow structures in zero pressure-gradient turbulent boundary layers at high Reynolds numbers. Eur J Mech Fluids 22:379–390. doi:10.1016/S0997-7546(03)00034-7
22. Piquet J (1999) Turbulent flows. Models and physics. Springer, Berlin, Germany, 761 pp
23. Rahman S (2002) Effect of bed roughness on scalar mixing in turbulent boundary layer. Ph.D. thesis, Georgia Institute of Technology, USA, 324 pp
24. Ralston DK, Stacey MT (2005) Stratification and turbulence in subtidal channels through intertidal mudflats. J Geophys Res Oceans, AGU, Vol. 110, Paper C08009, 16 pp
25. Rao KN, Narasimha R, Narayanan AAB (1971) The "bursting" phenomena in a turbulent boundary layer. J Fluid Mech 48(Part 2):339–352. doi:10.1017/S0022112071001605
26. Rudra Kumar S, Ameenulla S, Prabhu A (1995) MONTBLEX tower observations: instrumentation, data acquisition and data quality. Proc Indian Acad Sci (Earth Planet Sci) 104(2): 221–248
27. Sanvenije HHG (2005) Salinity and tides in alluvial estuaries. Elsevier, Amsterdam, The Netherlands, 194 pp
28. Shiono K, West JR (1987) Turbulent perturbations of velocity in the Conwy estuary. Estuar Coast Shelf Sci 25:533–553. doi:10.1016/0272-7714(87)90113-2
29. Stacey MT, Monismith SG, Burau JR (1999) Observations of turbulence in a partially stratified estuary. J Phys Oceanogr 29(Aug):1950–1970. doi:10.1175/1520-0485(1999)029<1950:OOTIAP>2.0.CO;2
30. Thorne PD, Vincent CE, Hardcastle PJ, Rehman S, Pearson N (1991) Measuring suspended sediment concentrations using backscatter devices. Mar Geol 98:7–16. doi:10.1016/0025-3227(91)90031-X
31. Trevethan M (2008) A fundamental study of turbulence and turbulent mixing in a small subtropical estuary. Ph.D. thesis, Department of Civil Engineering, The University of Queensland, 342 pp
32. Trevethan M, Chanson H, Takeuchi M (2007) Continuous high-frequency turbulence and sediment concentration measurements in an upper estuary. Estuar Coast Shelf Sci 73(1–2):341–350. doi:10.1016/j.ecss.2007.01.014
33. Trevethan M, Chanson H, Brown RJ (2007) Turbulence and turbulent flux events in a small subtropical estuary. Report No. CH65/07, Hydraulic Model Report series, Division of Civil Engineering, The University of Queensland, Brisbane, Australia, November, 67 pp
34. Trevethan M, Chanson H, Brown R (2008) Turbulent measurements in a small subtropical estuary with semi-diurnal tides. J Hydraul Eng 134(11):1665–1670. doi:10.1061/(ASCE)0733-9429(2008)134:11(1665)
35. Voulgaris G, Meyers ST (2004) Temporal variability of hydrodynamics, sediment concentration and sediment settling in a tidal creek. Cont Shelf Res 24:1659–1683. doi:10.1016/j.csr.2004.05.006